NJC

Accepted Manuscript

This is an *Accepted Manuscript*, which has been through the Royal Society of Chemistry peer review process and has been accepted for publication.

Accepted Manuscripts are published online shortly after acceptance, before technical editing, formatting and proof reading. Using this free service, authors can make their results available to the community, in citable form, before we publish the edited article. We will replace this *Accepted Manuscript* with the edited and formatted *Advance Article* as soon as it is available.

You can find more information about *Accepted Manuscripts* in the Information for Authors.

Please note that technical editing may introduce minor changes to the text and/or graphics, which may alter content. The journal's standard Terms & Conditions and the Ethical guidelines still apply. In no event shall the Royal Society of Chemistry be held responsible for any errors or omissions in this *Accepted Manuscript* or any consequences arising from the use of any information it contains.

ROYAL SOCIETY OF CHEMISTRY

www.rsc.org/njc

Journal Name

RSC Publishing

ARTICLE

Ultrasensitive detection of bisphenol A in aqueous media via photoresponsive surface molecular imprinting polymer microspheres

Cite this: DOI: 10.1039/x0xx00000x

Received 00th January 2012,
Accepted 00th January 2012

DOI: 10.1039/x0xx00000x

www.rsc.org/

Yu-zhu Yang,[a] Qian Tang,[a] Cheng-bin Gong,[a,*] Xue-bing Ma,[a,*] Jing-dong Peng,[a] Michael Hon-wah Lam[b]

Photoresponsive surface molecular imprinting polymer (SMIP) microspheres were synthesized on silica microspheres by surface polymerization using a water-soluble azobenzene-containing 4-[(4-methacryloyloxy)phenylazo]benzenesulfonic acid as the functional monomer. The SMIP microspheres displayed good photoresponsive properties and specific affinity to bisphenol A (BPA) with high recognition ability (maximal adsorption capacity: 6.96 μmol g^{-1}) and fast binding kinetics (binding constant: 2.47×10^4 M^{-1}) for BPA in aqueous media. Upon alternate irradiation at 365 and 440 nm, the SMIP microspheres could quantitatively uptake and release BPA. Analytical application of the SMIP microspheres for the detection of trace BPA concentration in mineral water and tap water has been carried out successfully, and therefore a simple and quick detection method for trace BPA in the environment was established.

Introduction

Bisphenol A (BPA) is extensively used as the monomer for the manufacture of polycarbonate plastics and epoxy resins, and therefore is included in various products such as nursing bottle, the resin lining of cans, mineral water bottle, beverage container, medical apparatus, food packaging bag etc. The global capacity of plastics containing BPA is about 2.7×10^7 ton/year.[1,2] However, the ester bonds in these BPA-based polymers are not stable, and are easily hydrolyzed especially at elevated temperatures, under acidic or basic conditions, or for extending periods of time, leading to leaching of BPA and widespread human exposure.[3-9] Because of the wide existence of BPA in the environment, the potential adverse effects of BPA on human health have caused a great concern. The risk assessment[1] and development of sensitive and selective detection methods for BPA in biological, water and soil matrices are of great importance and necessity. Many evidences have shown that BPA is a typical endocrine disruptor, which could potentially interfere with the endocrine system of wildlife and humans, increase cancer rate, reduce immune function, and impair reproduction.[1-3] Conventional methods such as high performance liquid chromatography (HPLC),[5,7,8] GC-MS,[6] electrochemical methods,[10,11] and fluorescence methods[12] have been used for the determination of BPA. Those methods are sensitive and highly specific, but expensive equipment, large volume of solvent, skillful operator as well as complicated clean up procedure are required. Therefore, it is of great necessity to develop efficient, selective, fast and inexpensive detection methods for the determination of trace BPA in real samples.

Molecular imprinting is well known as a technology for generating specific recognition sites with memory of the shape, size, and functionality of templates and possesses many promising characteristics such as desired selectivity, physical robustness, thermal stability, as well as low cost and easy preparation.[13] Therefore, molecularly imprinted polymers (MIPs) have been extensively used in separation processes, biotechnology, catalysis, and chemical sensors.[14-17] MIPs are mainly used as sorbents for solid-phase extraction of BPA from various samples.[18-22] In recent years, stimulus-responsive (especially magnetic field-responsive) MIPs have attracted much research attention.[23-28] Such magnetic MIPs have been used as a sorbent for selective adsorption of BPA in solution samples. The magnetic MIPs sorbent was then removed from the solution by applying an external magnetic field. Although remarkable achievements have been obtained in the molecular imprinting, there are still some challenges. (1) The research on other stimuli-responsive MIPs especially photoresponsive MIPs is scarce[29-46] except magnetic field stimulus. However, light is a clean stimulus, and light irradiation is manipulated precisely and rapidly. Compared with other MIPs, the analyte uptaked by photoresponsive MIPs is conveniently and efficiently released by a proper light irradiation in solution instead of eluting the analyte in a solution for longer time. (2) The molecular imprinting efficiency in conventional MIPs is not very good. Therefore, surface imprinting technique has been used to improve the efficiency.[35,36,43] (3) Furthermore, most of the reported MIPs only work in organic media, and fail to show specific binding in aqueous media,[29-33,35-39,47-50] To the best of our knowledge, only two research groups reported water-compatible MIP via different methods. Zhang research group[34] reported a water-compatible MIP microspheres by grafting

poly(NIPAAm) brushes to MIP microspheres. Our research group reported photoresponsive water-compatible molecularly imprinted hydrogels using water-soluble azobenzene-containing functional monomer.[41,43] Herein, we prepared photoresponsive surface molecular imprinting polymer (SMIP) microspheres on silica microspheres using a water-soluble azobenzene-containing 4-[(4-methacryloyloxy)phenylazo] benzenesulfonic acid (MAPASA) as the functional monomer for the photocontrolled ultrasensitive detection of trace BPA in aqueous media, and therefore developed a rapid and simple detection process for trace BPA in aqueous samples.

Experimental section

Materials

2,2-Azobisisobutyronitrile (AIBN) was recrystallized in methanol prior to use. Methacrylic chloride was synthesized from methacrylic acid and $SOCl_2$ (b.p. 96 – 98 ^oC, colorless oil). N,N-dimethylformamide (DMF, AR), 2-[4-(2-Hydroxyethyl)-1-piperazinyl]ethane sulfonic acid (HEPES, 99.0 %), [1,1'-biphenyl]-4,4'-diol (BiP, 97%), p-tertbutylphenol (TBP, 99.0%), 3,3',5,5'-tetrabromobisphenol A (TBBPA, 98.0%), ethylene glycol dimethacrylate (EGDMA) (AR), BPA (AR, 99.0%), vinyltriethoxysilane (AR), and tetraethoxysilane (TEOS, AR) were purchased from Aladdin Co., Shanghai, China. All solvents used were of analytical reagent grade in market sales. 0.01 mol L^{-1} HEPES (pH=7.20) buffer was used throughout the experiment.

Modification of silica microspheres

Uniform silica microspheres were synthesized according to Stöber method[51] by the hydrolysis of TEOS. The monodisperse silica microspheres were easily obtained by the centrifugation of the resultant white emulsion and then washed thoroughly with ethanol and deionized water, respectively.

Silica microspheres (1.20 g) were activated by refluxing in 30.0 mL of 10% hydrochloric acid for 12 h. The activated silica microspheres were obtained by centrifugation and then washed thoroughly with deionized water to neutral and finally dried under vacuum at 50 ^oC for 24 h.

Silica surface was modified according to a previous method[19] with some modification. Activated silica microspheres (0.40 g) in 50.0 mL of toluene were introduced to a dried 250 mL three-necked flask equipped with a mechanical stirrer, a thermometer, and a 25.0 mL dropping funnel. Vinyltriethoxysilane (2.20 mL) in 5.0 mL of toluene was introduced to the dropping funnel, and then added dropwise into the silica suspension within 15 min under stirring. 2.0 mL of aqueous ammonia was then added drop by drop. The resultant mixture was stirred for 24 h at room temperature. The product in the form of white powder (0.73 g, yield 30.4%) was collected by centrifugation and washed with toluene (8.0 mL × 4), and finally dried under vacuum at 50 ^oC for 24 h.

Preparation of photoresponsive SMIP microspheres

The functional monomer MAPASA (Fig. 1) was synthesized according to our previous report.[41] ^1H NMR (300 MHz, d_6–DMSO): δ 10.4 (1H, broad, SO_3H), 7.97 (d, 2H), 7.82 (dd, 4H), 7.42 (d, 2H), 6.32 (s, 1H), 5.94 (s, 1H), 2.01 (s, 3H).

To a 50 mL flask, the modified silica microspheres (0.30 g) were dispersed in 10.0 mL of DMF by ultrasonic stirring for 5 min. BPA (59.0 mg, 0.25 mmol), MAPASA (0.17 g, 0.5 mmol), EGDMA (0.50 g, 2.5 mmol), and deionized water (10.0 mL) were introduced. The mixture was ultrasonically stirred for another 5 min and then stored in dark for 12 h. After the addition of AIBN (100 mg), the resultant mixture was degassed by bubbling with N_2 for at least 20 min and sealed under N_2 atmosphere with a rubber cap. The mixture was then placed in an oil bath at 65 ^oC for 24 h. The BPA imprinted SMIP microspheres were obtained by centrifugation and dried under vacuum at 50 ^oC for 24 h. BPA in the photoresponsive SMIPs was removed by Soxhlet extraction with 200 mL of methanol/acetic acid mixture (9:1 v/v) for 48 h followed by 200 mL of methanol for 12 h in dark. The resultant SMIP was dried to constant weight under vacuum at 40 ^oC for 24 h. The surface non–imprinted molecular polymer (SNIP) was prepared in an identical fashion to the BPA–imprinted SMIP, with the only difference being that no BPA was used in the polymerization procedure. Both the SMIP and SNIP were stored at room temperature in the dark.

Characterization

^1H NMR (300 MHz) was performed on a Bruker AV–300NMR instrument at ambient temperature using TMS as an internal standard. UV–Vis spectra was recorded with UV–4802 Spectrophotometer (UNICO (Shanghai) Instruments Co. Ltd.). CEL–S500 Xe lamp (Beijing Zhongjiao jinyuan keji Co., Ltd.) was used as a light source. 365 and 440 nm light were selected by 365 and 440 nm filter, respectively. High performance liquid chromatography (HPLC) were measured by Agilent 1100 liquid chromatography (Agilent Technologies, CA, USA), 278 nm UV detector. Fourier Transform Infrared spectroscopy (FT–IR) was recorded on a Perkin–Elmer Model GX Spectrometer using a KBr pellet method. The surface morphologies of silica microspheres and SMIP were identified by scanning electron microscopy (SEM; S–4800, Hitachi, Tokyo, Japan). The diameter distributions of silica microspheres and SMIP were analyzed using a Laser Partical Size Analyzer (Jinan Rise Science and Technology co., Ltd, China).

To investigate the binding kinetics of the SMIP, 15.0 mg SMIP was incubated in 2.0 mL of 6.0×10^{-5} mol L^{-1} BPA solution (methanol: HEPES buffer with a volume ratio of 2 : 98) in the dark at 25 ^oC, and sampled at different intervals. The amounts of BPA bound to the SMIP/SNIP microspheres were then quantified with HPLC equipped with a UV–Vis detector. The wavelength used for the determination of BPA was 278 nm. A mixture of methanol and water with a volume ratio of 80/20 was used as the mobile phase at a flow rate of 0.40 mL min^{-1}.

Binding properties of the SMIP was studied by batch–type rebinding assays by incubating 15.0 mg SMIP in 2.0 mL solution (methanol: HEPES buffer with a volume ratio of 2 : 98) with different amount of BPA at room temperature and agitated for 24 h. Each of the suspensions was then filtered with 0.22 μm porous membrane. The amount of BPA left after rebinding was determined by HPLC. The HPLC was calibrated using standard BPA solutions with concentration ranging from 0 to 2.0×10^{-4} mol L^{-1}. The equilibrium adsorption capacity of BPA (Q) by SMIP was calculated according to the Scatchard equation (1),[52]

$$\frac{Q}{c_{BPA}} = \frac{Q_{max} - Q}{K_d} \qquad (1)$$

where C_{BPA} is the equilibrium concentration of BPA, Q_{max} is the apparent maximum adsorption capacity, and K_d is the binding constant.

In order to estimate the selectivity of SMIP to BPA, structural analogs (TBP, BiP, and TBBP) were used as competitive compounds (Fig. 1). The procedure was similar to Refs. 40-45. The level of BPA, TBP, Bip, and TBBP in the solution was monitored by HPLC.

All photocontrolled release and uptake of the analyte BPA by SMIP were performed by alternate irradiation with 365 and 440 nm light. In all experiments, 30.0 mg of SMIP in 3.0 mL of solution was used. All of the initial concentration of BPA, TBP, BiP, and TBBP were 6.0×10^{-5} mol L^{-1}. The suspension was stirred in dark for 12 h. For the photocontrolled release of BPA, TBP, BiP, and TBBP, the mixture was stirred and irradiated at 365 nm for 1 h. The stirring was then stopped and the mixture was allowed to settle for 3 min in darkness before 50.0 μL of the clear supernatant solution was taken out by a clean gas–tight HPLC syringe and filtered through 0.22 μm micro-porous membrane. The level of BPA in the solution was monitored by HPLC. Stirring and irradiation was resumed after the sampling of supernatant. Each round of irradiation was 60 min and substrate concentration in the solution and the UV–Vis absorbance change were measured at the end of each irradiation round. For the photocontrolled uptake of substrate, irradiation at 440 nm for 60 min was adopted. Besides this, all procedures were similar to those in the release experiments.

Effect of BPA concentration on the isomerization rate of azobenzene in SMIP was studied as follows: In all experiments, 10.0 mg of SMIP material in 25.0 mL deionized water was used as the SMIP sample. A known amount of BPA (2.0×10^{-6}, 3.0×10^{-6}, 4.0×10^{-6}, 6.0×10^{-6}, 8.0×10^{-6}, 9.0×10^{-6}, 1.0×10^{-5}, 2.0×10^{-5}, 2.5×10^{-5}, 3.0×10^{-5}, 4.0×10^{-6}, 6.0×10^{-5}, 8.0×10^{-5}, 10.0×10^{-5} mol L^{-1}, respectively, containing 2.0% methanol and 98.0% deionized water) was added to 1.5 mL SMIP sample, the suspension was then diluted with deionized water to 3.0 mL and stirred in the dark for 24 h before UV–Vis analysis.

Analytical application of the SMIP for the direct detection of BPA in mineral water and tap water was examined. The mineral water was purchased from a local supermarket. No BPA has been detected in both the tap water and the mineral water by UV–Vis analysis. BPA spiked mineral and tap water samples were prepared by spiking known amount of BPA into mineral water and tap water with BPA concentration of 0, 0.5, 0.6, 1.0, and 5.0 ppm, respectively. Then the spiked water sample was mixed with 1.5 mL SMIP suspensions (v:v = 1:1), and the resultant suspension was stirred in the dark for 24 h before UV–Vis analysis.

Results and Discussion

Preparation of SMIP

A non–covalent molecular imprinting approach was used to prepare the SMIP, and the synthetic route of the SMIP is shown in Fig. 2.

Main factors (such as the amount of template, the percentage of functional monomer and cross-linker, the type and the percentage of porogenic solvent, molar ratio of modified silica/monomer, amounts of initiator, reaction temperature, and reaction time) that affect the SMIP structure and its molecular recognition properties have been optimized. The optimum conditions were as follows: mixture of water and DMF (1:1, v/v) as the porogenic solvent, modified silica/monomer with a mass ratio of 1.5:1, cross–linker/monomer with a molar ratio of 5:1.

Characterization of SMIP

The morphologies of silica microspheres and SMIP microspheres have been observed by SEM (Fig. 3). The size of the silica microspheres was about 720 nm in diameter with good size mono–disperse and smooth surface (Fig. 3A). The diameter of SMIP increased to about 800 nm after surface imprinting (Fig. 3B), and the surface became much rougher. It could be concluded that SMIP has been prepared successfully via precipitation polymerization. The result of particle size analysis was consistent with SEM investigation (Fig. 3C).

The modified silica and SMIP were further verified via FT-IR. Fig. 4 presents the FT-IR spectra of silica, modified silica, and SMIP microspheres. The adsorption observed at 1604 and 1430 cm^{-1} indicates the existence of -C=C- group in the modified silica microspheres.[19] The appearance of an adsorption at 1748 and 1500–1600 cm^{-1} indicates the existence of C=O group of monomer and C-H stretching frequency of benzene ring in SMIP.

The thermostability of SMIP was characterized by thermo-gravimetric analysis (TGA). Fig. 5 shows TGA of the silica (curve a), modified silica (curve b), and SMIP (curve c). In curve a, the 5% weight loss below 150 ^{o}C could be ascribed to the adsorbed water on silica surface, and the further 3% weight loss was probably caused by desorption of water from Si–OH. In curve b, the 5% weigh loss below 150 ^{o}C could also be attributed to the removal of physically adsorbed water, and the further 5.9% weight loss beyond 350°C could be attributed to the decomposition of C=C organic skeleton on silica surface. In curve c, similarly, the 10.5% weight loss between 100–300 ^{o}C could be ascribed to the removal of adsorbed water and the desorption water from Si–OH, the further 46.2% weight loss within the temperature range of 350–600 ^{o}C was probably caused by the removal of the organic content in the surface imprinted layer, which further proved that organic functional monomer was successful grafted on the surface of silica. This result also illustrates that SMIP is more thermostable than conventional organic-based MIP.[46]

Photoisomerization analysis of SMIP

Photoisomerization of the azobenzene chromophore in the SMIP microspheres was studied in HEPES aqueous buffer by UV–Vis. Fig. 6 shows the spectroscopic responses of SMIP at room temperature upon alternate irradiation at 365 and 440 nm. It was found that irradiating SMIP at 365 nm caused the drop of the absorption peak at 331 nm (Fig. 6A). This is attributable to the *trans*→*cis* photoisomerization of the azobenzene. The photo–stationary state was reached after 44 min of irradiation at 365 nm. Subsequent irradiation at 440 nm caused the reverse *cis*→*trans* photoisomerization to recovery (Fig. 6B), which was typical for the azobenzene compounds and could be ascribed to the $\pi\rightarrow\pi^*$ electron transitions of the *N*=*N* bond. Kinetic rate constants for *trans*→*cis* and *cis*→*trans* isomerization were calculated to be $(1.37 \pm 0.02) \times 10^{-3}$ s^{-1} and $(9.83 \pm 1.14) \times 10^{-3}$ s^{-1}. Compared with isomerization rate constants of MAPASA monomer ($(2.42 \pm 0.04) \times 10^{-3}$ s^{-1}, $(12.5 \pm 0.10) \times 10^{-3}$ s^{-1}), both the *trans*→*cis* and *cis*→*trans* photoisomerization rates of SMIP were smaller than that of MAPASA in solution.[46] The results illustrated that photoisomerization behavior was hindered to some degree after MAPASA was incorporated into the cross–linked poly–ethylene glycol dimethyl acrylate matrices. And the rigid 3–D network created by the cross–linker around the sulfonated azobenzene chromophores produced steric hindrance to the conformational switching of the azobenzene chromophores.

Reversibility of photoisomerization of the azobenzene chromophores within SMIP is an important factor for photoresponsive materials. Fig. 7 shows the modulation of the absorbance of SMIP upon alternate irradiation at 365 nm and 440 nm, no obvious change in absorbance at 331 nm was observed after 8 cycles, illustrating that the photoisomerization of the azobenzene chromophores within SMIP is reversible and robust.[41,44]

SMIP binding properties

The binding kinetics of the SMIP and SNIP was studied via incubating SMIP and SNIP in 2.0 mL of 6.0×10^{-5} mol L^{-1} BPA aqueous solution in the dark at 25 °C. Fig. 8 shows the binding kinetics of BPA on SMIP and SNIP versus the incubation time. For SMIP, binding amounts of BPA rapidly increased in the adsorption capacity within 40 min, and the equilibrium was obtained in 2 h with a binding capacity of about 73.0 %. For SNIP, the time to reach the equilibrium was much longer (4 h) and the binding capacity was much less (about 32.0 %). Namely, SMIP exhibited a much higher binding capacity and faster mass transfer rate than SNIP. This phenomenon could be explained as follows: The existence of more effective binding sites on the SMIP surface facilitated the BPA to diffuse into the SMIP pore rapidly during rebinding and allowed more BPA molecules bound on the surface. Compared with traditional MIP that cost long time to achieve the equilibrium,[53,54] this SMIP had faster transfer rate to BPA.

To further evaluate the specificity of SMIP for BPA, the photoregulated release and uptake of TBBPA, TBP, and BiP, whose structures are analogous to BPA (Fig. 1), by the SMIP were studied. Fig. 9 illustrates the absorption efficiency of BPA and its structural analogs by SMIP and SNIP. It was found that SMIP exhibited higher binding capacities toward BPA than its analogs. The adsorption capacity of BPA, BiP, TBP, and TBBPA were 71.0%, 29.2%, 22.8%, and 13.3%, respectively. For BiP, the adsorption capacity was a little higher than TBP and TBBPA due to its extremely similar structure to BPA, demonstrating a higher selectivity of the SMIP toward the template. The results illustrated that the recognition mechanism of SMIP was based on the interaction of size, shape, and functionality to the template.[55] For SNIP, there were no tailor–made recognition sites, and therefore the template molecules adsorbed on SNIP were less than those on SMIP. BPA-SMIP exhibited high selectivity and high affinity for BPA due to the template-specific sites, which was beneficial for separation and detection of BPA in sample system.

Fig. 10 illustrates Scatchard plot of the batch-type rebinding assay of SMIP with BPA. There are two straight lines in the graph, indicating the presence of two different binding sites for BPA on SMIP surface: specific binding and non-specific binding. The specific binding constant K_a and the binding density Q_{max} were calculated to be 2.47×10^4 M^{-1} and 6.96 μmol g^{-1} SMIP, respectively.

Photo − regulated release and uptake of BPA with SMIP

SMIP shows specific affinity to BPA. Fig. 11 illustrates the change in the amount of bound BPA and its structural analogs, TBP, BiP, and TBBPA in HEPES buffer in the presence of SMIP under alternate irradiation at 365 and 440 nm. SMIP showed significantly higher binding capacity toward BPA than its structural analogs. In total, 129.4 nmol of BPA was adsorbed from the aqueous solution into the SMIP. Namely, 71.9 % of the imprinted receptors in the SMIP were filled with BPA. Irradiation at 365 nm caused an obvious release of 25.4 nmol BPA from the SMIP into solution. After the equilibrium state was reached, the fraction of bound receptors in the SMIP was reduced to 57.8 %. This photoregulated release of bound BPA could be attributed to the photoinduced *trans→cis* isomerization of azobenzene chromophores in the SMIP receptor sites, resulting in a change in the receptor configuration.[46,48] Subsequent irradiation at 440 nm caused the uptake of 25.2 nmol BPA back into the SMIP, and the fraction of occupied receptor sites increased from 57.8 to 71.8 % in 90 min. In other words, the amount of rebound BPA was 99.2% of the BPA that had been previously released into solution. This near-quantitative uptake of the released BPA is evidence of the reversibility of the receptor-site configuration and substrate affinity in the course of photoswitching of the azobenzene chromophores. Repeating the 365–440 nm irradiation cycle resulted in the release and uptake of BPA in quantities very similar to those of the previous cycle. For its structural analogs, smaller values were obtained under similar experimental conditions. This demonstrates the substrate–specificity of the imprinted receptor sites in the SMIP for BPA. The binding capacity decreased in the order: Bip > BPP > TBBPA. This can be attributed to the difference in their chemical structures. The chemical whose chemical structure is more similar to BPA, its binding capacity is much larger.

Analytical application for the determination of trace BPA in real samples

It was found that the isomerization rate of azobenzene chromophores depended on BPA concentration. Fig. 12A illustrates the relationship between BPA concentration and isomerization rate of azobenzene in SMIP. Generally, as BPA concentration increased, isomerization rate of SMIP decreased due to the entrance of BPA into the cavities of SMIP.[46] It is interesting that two linear relationships between BPA concentration (0-2.30 ppm and 2.3-23.0 ppm) and isomerization rate of azobenzene chromophores in SMIP have been obtained. And the photoisomerization rate was more sensitive at lower BPA concentration. Therefore, this curve was used as the standard curve for the indirect determination of BPA concentration in real samples by simply detecting the t*rans→cis* photoisomerization rate of the azobenzene moieties within the SMIP.

Analytical application of the SMIP for the determination of trace BPA in spiked tap water and mineral water was used to evaluate the feasibility of this method. Fig. 12B demonstrates that the *trans→cis* photoisomerization rates of both spiked mineral water and spiked tap water samples approximate to the corresponding standard samples, illustrating this method is effective. Furthermore, this method is simpler and faster than other methods,[7–12] which can be easily used for the detection of trace BPA in real samples with a limit of detection about 0.5 ppm. This value is lower than the standard values of BPA limited by European Union (2011/03/01 the European Union amended 2002/72/EC, BPA allow migration amount shall not be higher than 0.6 ppm) and Japan (2.5 ppm), denoting that this detection system can be used for the ultrasensitive determination of BPA concentration in environment and justify whether it exceeds the reference standard or not.

Conclusions

A photoresponsive SMIP material was prepared for the detection of trace BPA in aqueous media. The SMIP combined

many attractive characteristics such as uniform morphology, photoresponsive properties, higher binding capacity, as well as selective recognition. This detection method was simple, effective and sensitive with a limit of detection about 0.5 ppm, and therefore can be used to determine trace BPA concentration in real samples to justify whether it exceeds the reference standard or not.

Acknowledgments

This work was supported by the National Natural Science Foundation of China (20872121), CQ CSTC 2013jcyjA50026, Research Funds for the Doctoral Program of Higher Education of China (20090182120010), and Southwest University Doctoral Fund (SWUB2008075).

Notes and references

[a] The Key Laboratory of Applied Chemistry of Chongqing Municipality, College of Chemistry and Chemical Engineering, Southwest University, Chongqing, 400715, China. gongcbtq@swu.edu.cn, zcj123@swu.edu.cn
[b] Department of Biology & Chemistry, City University of Hong Kong, Hong Kong, China.

† Footnotes should appear here. These might include comments relevant to but not central to the matter under discussion, limited experimental and spectral data, and crystallographic data.

Electronic Supplementary Information (ESI) available: [details of any supplementary information available should be included here]. See DOI: 10.1039/b000000x/

1 F. S. vom Saal, C. Hughes, *J. Environ. Health Persp*., 2005, **113**, 926.
2 Y. B. Wetherill, C. E. Petre, K. R. Monk, A. Puga, K. E. Knudsen, *Mol. Cancer. Ther*., 2002, **1**, 515.
3 M. Muno–zde–Toro, C. M. Markey, P. R. Wadia, E. H. Luque, B. S. Rubin, C. Sonnenschein, A. M. Soto, *Endocrinology*, 2005, **146**, 4138.
4 M. Telscher, U. Schuller, B. Schmidt, A. Schaffer, *Environ. Sci. Technol*., 2005, **39**, 7896.
5 Y. Watabe, T. Kondo, M. Morita, N. Tanaka, J. Haginaka, K. Hosoya, J. *Chromatogr. A*, 2004, **1032**, 45.
6 M. Kawaguchi, K. Inoue, M. Yoshimura, R. Ito, N. Sakui, N. Okanouchi, H. Nakazawa, *J. Chromatogr. B*, 2004, **805**, 41.
7 K. Inoue, K. Kato, Y. Yosh, H. Nakazawa, *J. Chromatogr. B,* 2000, **749**, 17.
8 R. S. Zhao, X. Wang, J. P. Yuan, L. L. Zhang, *Microchim Acta*, 2009, **165**, 443.
9 J. Z. Liu, W. Z. Wang, Y. F. Xie, Y. Y. Huang, Y. L. Liu, X. J. Liu, R. Zhao, G. Q. Liu, Y. Chen, *J. Mater. Chem*., 2011, **21**, 9232.
10 H. S. Yin, Y. L. Zhou, S. Y. Ai, Q. P. Chen, X. B. Zhu, X. G. Liu, L. S. Zhu, *J. Hazard. Mater.*, 2010, **174**, 236.
11 F. R. Wang, J. Q. Yang, K. B. Wu, *Anal. Chim. Acta*., 2009, **638**, 23.
12 X. Wang, H. L. Zeng, L. X. Zhao, J. M. Lin, *Anal. Chim. Acta*., 2006, **556**, 313.
13 L. X. Chen, S. F. Xu, J. H. Li, *Chem. Soc. Rev*., 2011, **40**, 2922.
14 A. Kikuchi, T. Okano, *Prog. Polym. Sci.*, 2002, **27**, 1165.
15 P. S. Stayton, T. Shimoboji, G. Long, A. Chilkoti, G. H. Chen, J. M. Harris, A. S. Hoffman, *Nature*, 1995, **378**, 472.
16 M. Tada, Y. Iwasawa, *J. Mol. Catal. A: Chem.*, 2003, **199**, 115.
17 C. M. Ruan, K. F. Zheng, C. A. Grimes, *Anal. Chim. Acta*, 2003, **497**, 123.
18 R. Zhu, W. H. Zhao, M. J. Zhai, F. D. Wei, Z. Cai, N. Sheng, Q. Hu, *Anal. Chim. Acta*, 2010, **658**, 209.
19 W. H. Zhao, N. Sheng, R. Zhu, F. D. Wei, Z. Cai, M. J. Zhai, S. H. Du, Q. Hu, *J. Hazard. Mater*., 2010, **179**, 223.
20 X. H. Wang, L. R. Chen, X. J. Xu, Y. Z. Li, *Anal. Bioanal. Chem*., 2011, **401**, 1423.
21 D. K. Alexiadou, N. C. Maragou, N. S. Thomaidis, G. A. Theodoridis, M. A. Koupparis, *J. Sep. Sci*., 2008, **31**, 2272.
22 Y. M. Ren, W. Q. Ma, J. Ma, Q. Wen, J. Wang, F. B. Zhao, *J. Colloid Interf. Sci.*, 2012, **367**, 355.
23 Z. Xu, L. Ding, Y. J. Long, L. G. Xu, L. B. Wang, C. L. Xu, *Anal. Methods*, 2011, **3**, 1737.
24 Y. Li, X. Li, J. Chu, C. K. Dong, J. Y. Qi, Y. X. Yuan, *Environmental Pollution*, 2010, **158**, 2317.
25 J. Z. Liu, W. Z. Wang, Y. F. Xie, Y. Y. Huang, Y. L. Liu, X. J. Liu, R. Zhao, G. Q. Liu, Y. Chen, *J. Mater. Chem*., 2011, **21**, 9232.
26 J. M. Pan, W. Hu, X. H. Dai, W. Guan, X. H. Zou, X. Wang, P. W. Huo, Y. S. Yan, *J. Mater. Chem.*, 2011, **21**, 15741.
27 N. Griffete, H. Li, A. Lamouri, C. Redeuilh, K. Chen, C. Z. Dong, S. Nowak, S. Ammar, C. Mangeney, *J. Mater. Chem*., 2012, **22**, 1807.
28 Z. K. Lin, W. J. Cheng, Y. Y. Li, Z. R. Liu, X. P. Chen, C. J. Huang, *Anal. Chim. Acta*, 2012, **720**, 71.
29 M. Yamada, M. Kondo, J. I. Mamiya, Y. Yu, M. Kinoshita, C. J. Barrett, T. Ikeda, *Angew. Chem. Int. Ed.*, 2008, **47**, 4986.
30 N. Minoura, K. Idei, A. Rachkov, Y. W. Choi, M. Ogiso, K. Matsuda, *Macromolecules*, 2004, **37**, 9571.
31 T. Takeuchi, K. Akeda, S. Murakami, H. Shinmori, S. Inoue, W. S. Lee, T. Hishiya, *Org. Biomol. Chem*., 2007, **5**, 2368.
32 C. Gomy, A. R. Schmitzer, *Org. Lett.*, 2007, **9**, 3865.
33 L. J. Fang, S. J. Chen, Y. Zhang, H. Q. Zhang, *J. Mater. Chem*., 2011, **21**, 2320.
34 L. J. Fang, S. J. Chen, X. Z. Guo, Y. Zhang, H. Q. Zhang, *Langmuir*, 2012, **28**, 9767.
35 D. S. Wang, X. X. Zhang, S. Q. Nie, W. F. Zhao, Y. Lu, S. D. Sun, C. S. Zhao, *Langmuir*, 2012, **28**, 13284.
36 D. S. Wang, D. Y. Xie, W. B. Shi, S. D. Sun, C. S. Zhao, *Langmuir*, 2013, **29**, 8311.
37 X. R. Zhou, S. A. Zhong, G. S. Jiang, *Polym. Int*., 2012, **61**, 1778.
38 G. S. Jiang, S. A. Zhong, L. Chen, I. Blakey, A. Whitaker, *Radiation Physics and Chemistry*, 2011, **80**, 130.
39 X. J. Li, S. A. Zhong, C. E. Li, *J. Appl. Polym. Sci*., 2013, **130**, 869.
40 C. B. Gong, M. H. W. Lam, H. X. Yu, *Adv. Func. Mate*r., 2006, **16**, 1759.
41 C. B. Gong, K. L. Wong, M. H. W. Lam, *Chem. Mater.,* 2008, **20**, 1353.
42 Q. Tang, Y. T. Nie, C. B. Gong, C. F. Chow, J. D. Peng, M. H. W. Lam, *J. Mater. Chem*., 2012, **22**, 19812.
43 Q. Tang, C. B. Gong, M. H. W. Lam, X. K. Fu, *J. Sol-Gel Sci. Technol*., 2011, **59**, 495.
44 C. B. Gong, Y. Z. Yang, C. Gao, Q. Tang, C. F. Chow, J. D. Peng, M. H. W. Lam, *J. Sol-Gel Sci. Technol*., 2013, **67**, 442.
45 Q. Tang, C. B. Gong, M. H. W. Lam, X. K. Fu, *Sens. Actuator. B*, 2011, **156**, 100.

46 Q. Tang, X. Z. Meng, H. B. Jiang, T. Y. Zhou, C. B. Gong, X. K. Fu, S. Q. Shi, *J. Mater. Chem*., 2010, **20**, 9133.
47 H. Zhou, Y. P. Xu, H. W. Tong, Y. X. Liu, F. Han, X. Y. Yan, S. M. Liu, *J. Appl. Polym. Sci*., 2013, **128**, 3846.
48 K. G. Yang, Z. B. Liu, M. Mao, X. H. Zhang, C. S. Zhao, N. Nishi, *Anal. Chim. Acta*, 2005, **546**, 30.
49 S. Sasaki, T. Ooya, T. Takeuchi, *Polym. Chem.*, 2010, **1**, 1684.
50 Y. Kim, J. B. Jeon, J. Y. Chang, *J. Mater. Chem.,* 2012, **22**, 24075.
51 W. Stöber, A. Finker, E. J. Bohn, *Colloid Interf. Sci*., 1968, **26**, 62.
52 H. Zhou, Y. P. Xu, H. W. Tong, Y. X. Liu, F. Han, X. Y. Yan, S. M. Liu, *J. Appl. Polym. Sci*., 2012, **128**, 3846.
53 D. S. Wang, Q. Wei, Y. J. Zhang, C. S. Zhao, *J. App. Polym. Sci*., 2009, **114**, 4036.
54 K. G. Yang, J. J. Ma, H. Zhou, B. Q. Li, B. Y. Yu, C. S. Zhao, *Desalination*, 2009, **224**, 532.
55 Y. S. Chang, T. H. Ko, T. J. Hsu, M. J. Syu, *Anal. Chem.*, 2009, **81**, 2098.

Figures and Figure Captions

Fig. 1 Chemical structural of MAPASA, BPA, TBBPA, TBP, and Bip.
Fig. 2 Schematic procedure for the preparation of SMIP microspheres.
Fig.3 SEM microphotographs of silica microspheres (A) and SMIP microspheres (B). Particle diameter distribution of silica microspheres and SMIP from a Laser Partical Size Analyer (C) .
Fig. 4 FT-IR spectra of silica, modified silica, and SMIP microspheres.
Fig.5 Thermogravimetric curves of silica microspheres (curve a), the modified silica microspheres (curve b), and the SMIP (curve c).
Fig. 6 UV–Vis spectra and spectral changes of SMIP in 0.2 mg mL^{-1} HEPES buffer at pH 7.20 upon (A) irradiation at 365 nm, and then upon (B) irradiation at 440 nm. Insets: the kinetics of the photoisomerization of SMIP.
Fig.7 Reversibility of the photoisomerization processes of the azobenzene chromophores in the SMIP (0.2 mg mL^{-1} HEPES buffer pH=7.20) upon alternate irradiation at 365 and 440 nm, respectively.
Fig.8 Binding kinetics of BPA on SMIP and SNIP.
Fig.9 Absorption efficiency of BPA and its structural analogs.
Fig.10 Substrate binding properties of the SMIP to BPA.
Fig.11 Photoregulated release and uptake of BPA, TBP, BiP, and TBBPA by SMIP.
Fig.12 Photoisomerization rate of SMIP versus BPA concentration (A). The relationship between the photoisomerization rate of SMIP (in standard sample, mineral water and tap water samples) and the BPA concentration from 0, 0.5, 0.6, 1.0, and 5.0 ppm (B).

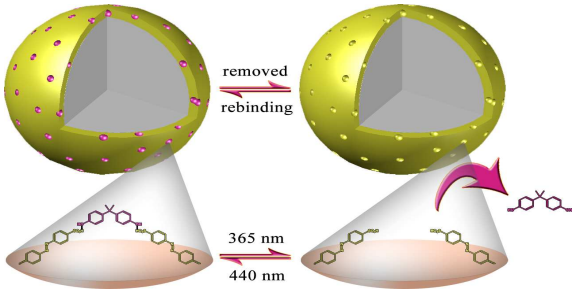

A photoresponsive SMIP was prepared for photocontrolled detection of trace bisphenol A in aqueous media with simplicity and good efficiency.

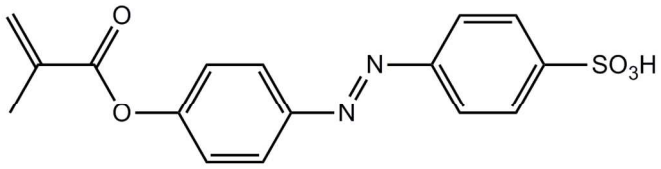

4-[(4-Methacryloyloxy)phenylazo]benzenesulfonicacid
MAPASA

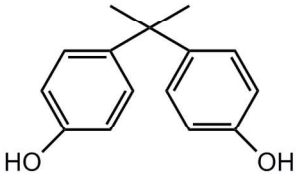

4,4'-(propane-2,2-diyl)diphenol
BPA

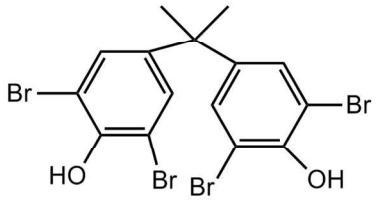

4,4'-(propane-2,2-diyl)bis(2,6-dibromophenol)
TBBPA

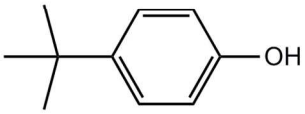

4-(*tert*-butyl)phenol
TBP

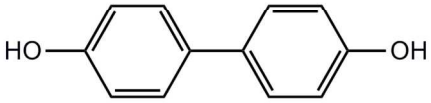

[1,1'-biphenyl]-4,4'-diol
BiP

Chemical structural of MAPASA, BPA, TBBPA, TBP, and Bip.
138x117mm (300 x 300 DPI)

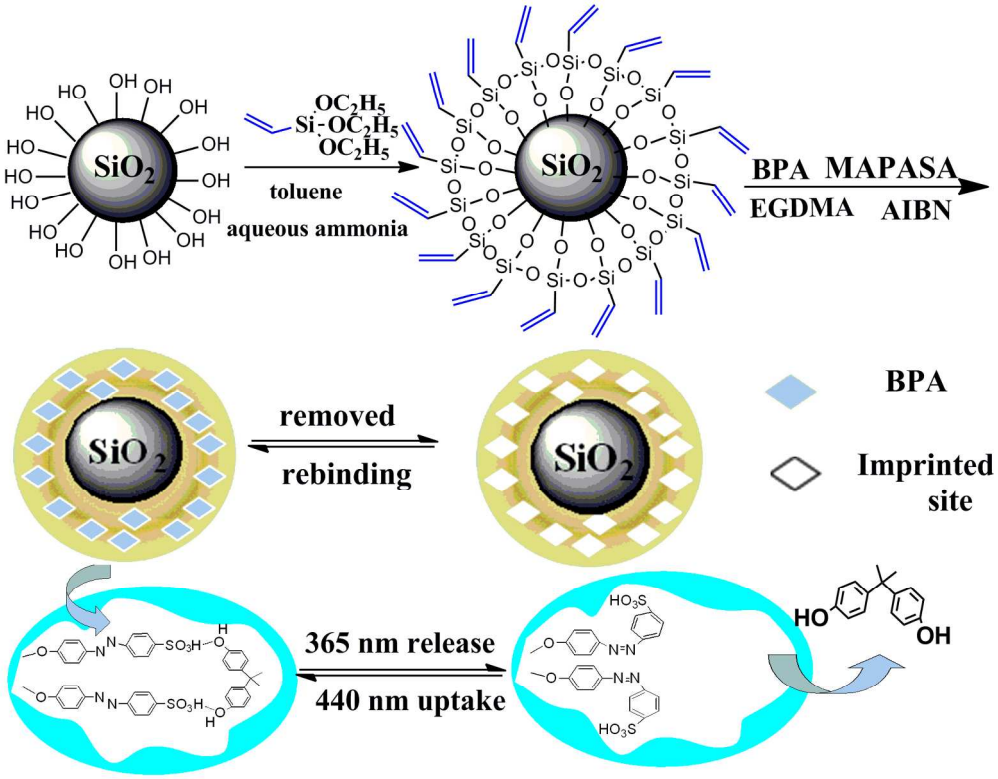

Schematic procedure for the preparation of SMIP microspheres.
179x140mm (300 x 300 DPI)

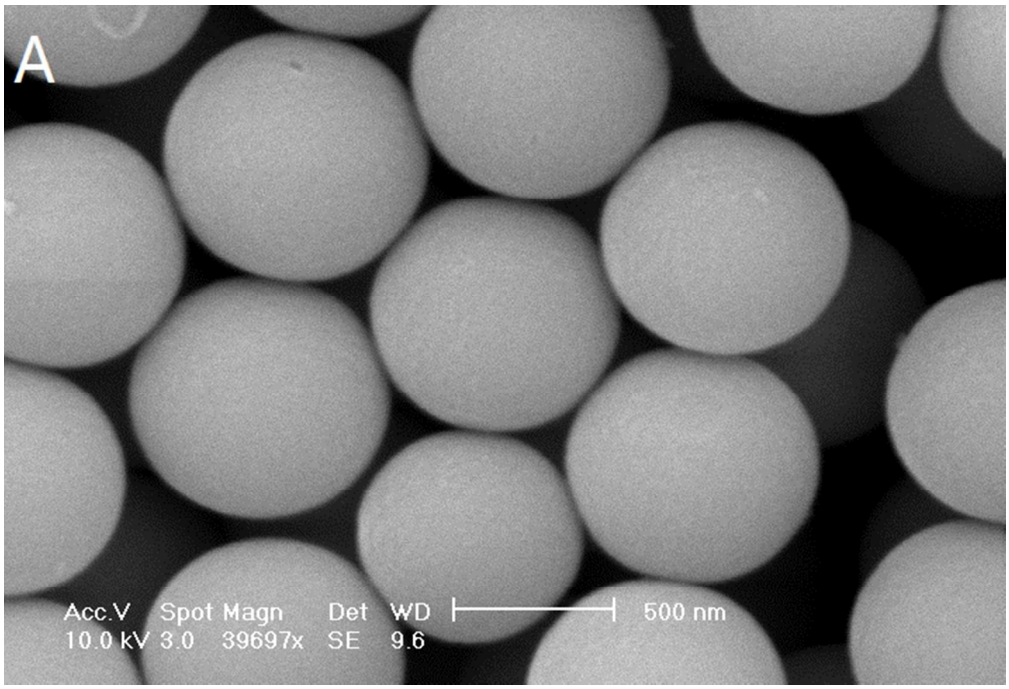

SEM microphotographs of silica microspheres

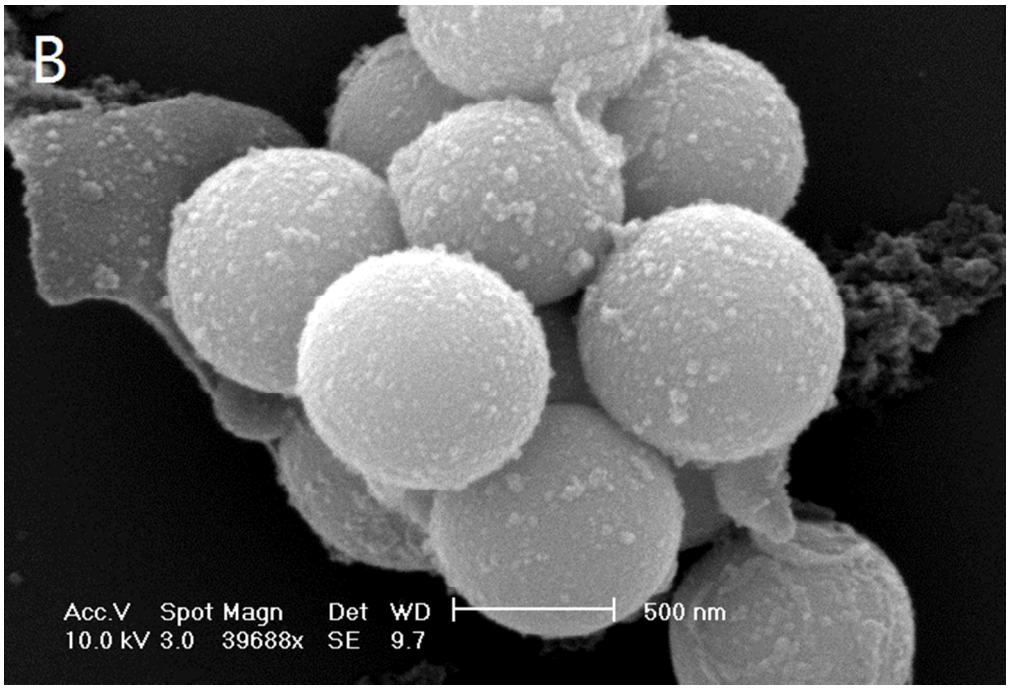

SEM microphotographs of SMIP microspheres

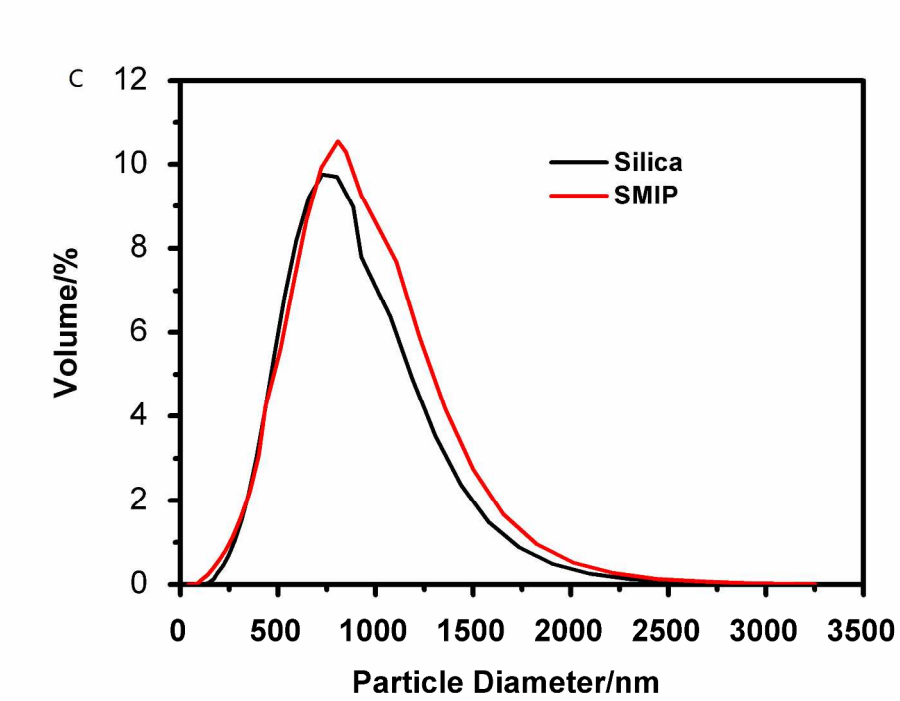

Particle diameter distribution of silica microspheres and SMIP from a Laser Partical Size Analyer

297x208mm (300 x 300 DPI)

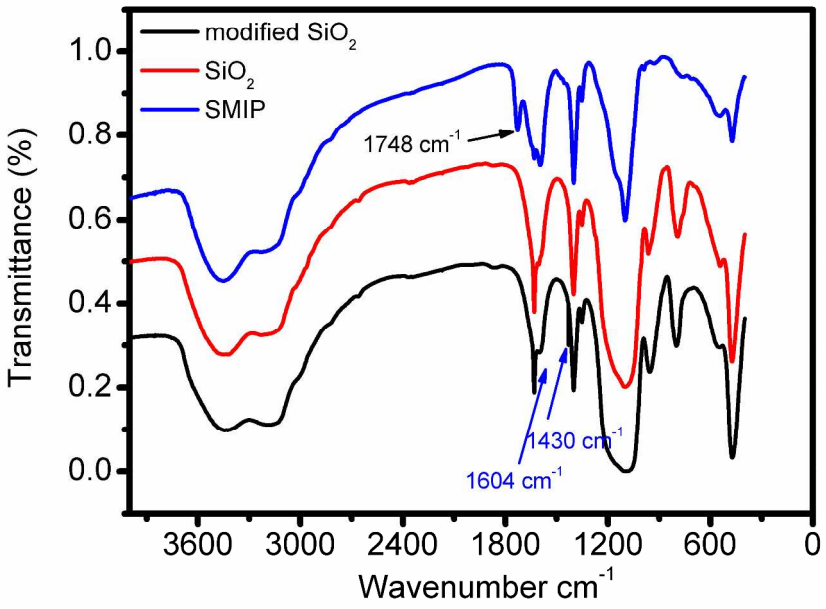

FT-IR spectra of silica, modified silica, and SMIP microspheres.
297x208mm (300 x 300 DPI)

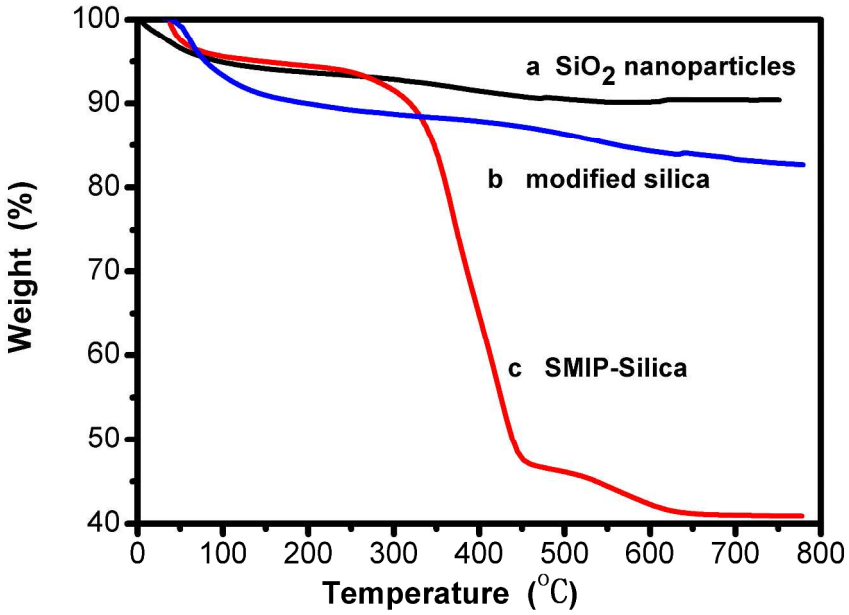

Thermogravimetric curves of silica microspheres (curve a), the modified silica microspheres (curve b), and the SMIP (curve c).

297x208mm (300 x 300 DPI)

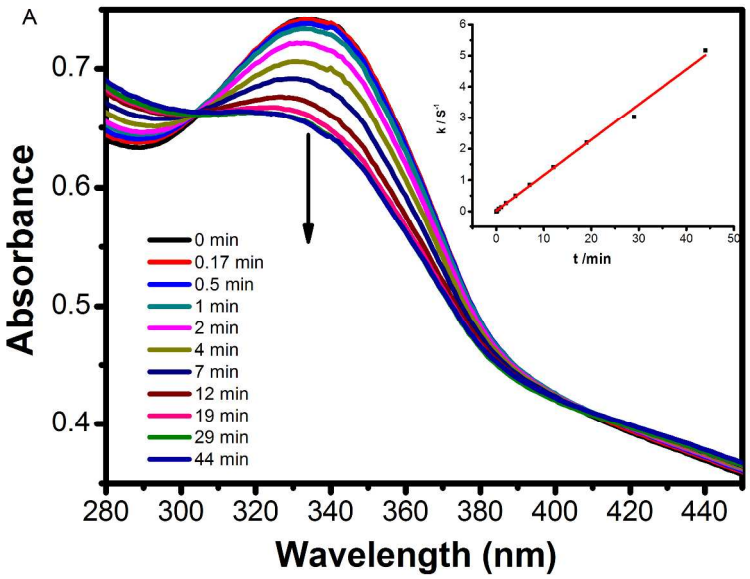

297x210mm (300 x 300 DPI)

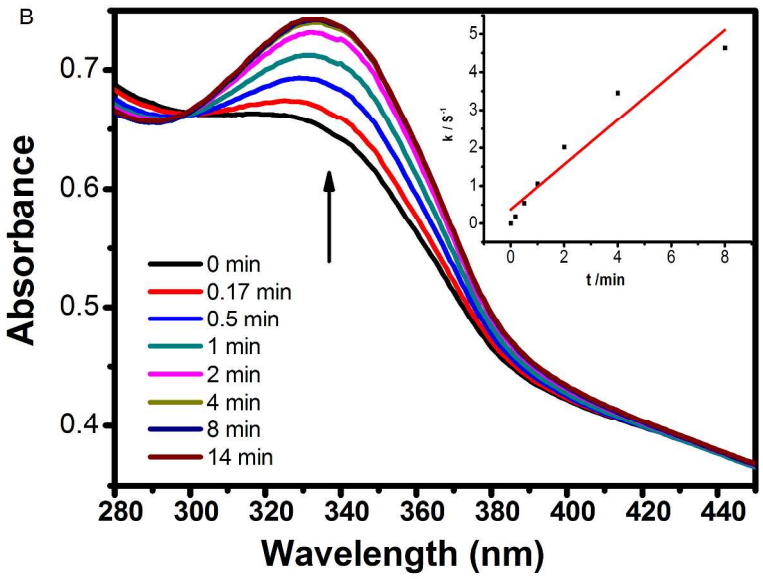

297x210mm (300 x 300 DPI)

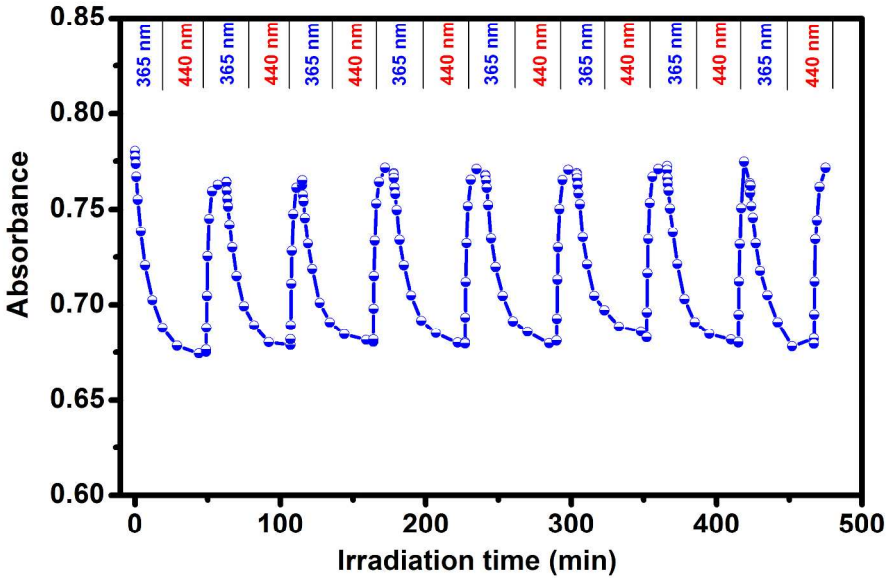

297x209mm (300 x 300 DPI)

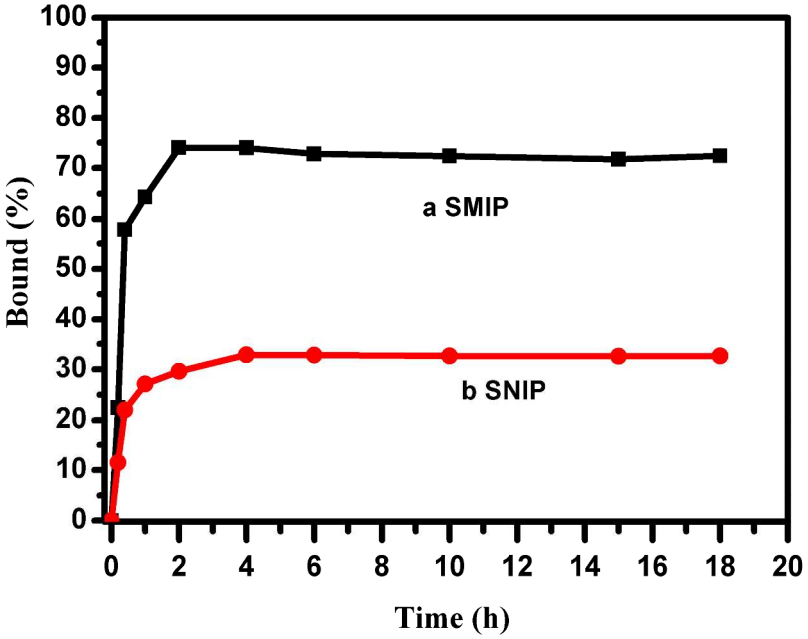

Binding kinetics of BPA on SMIP and SNIP.
297x208mm (300 x 300 DPI)

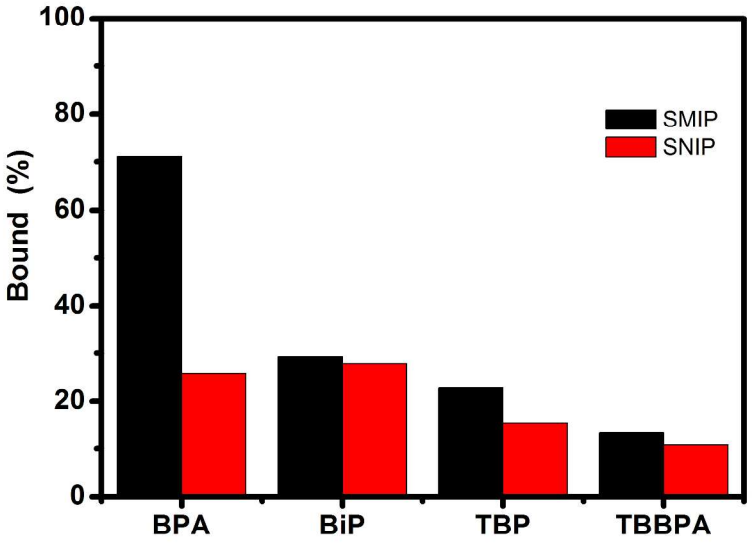

297x209mm (300 x 300 DPI)

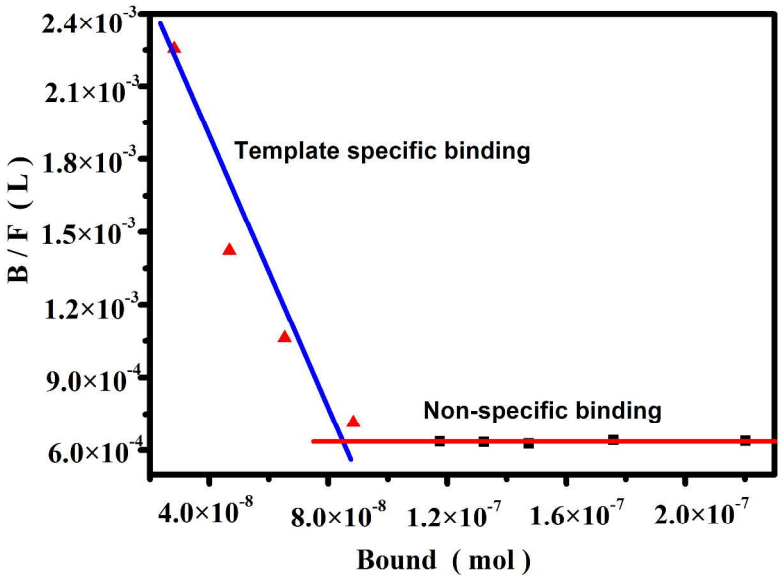

286x201mm (300 x 300 DPI)

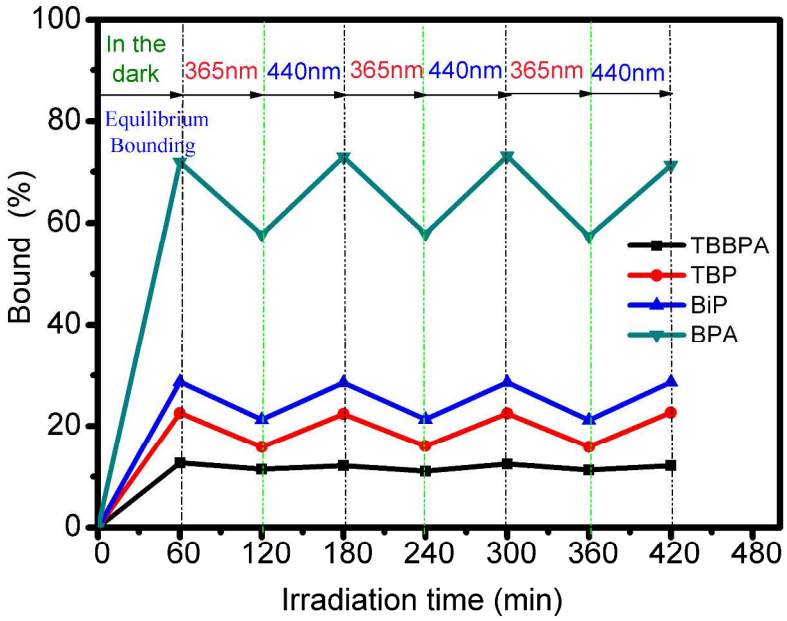

Binding kinetics of BPA on SMIP and SNIP.
297x210mm (300 x 300 DPI)

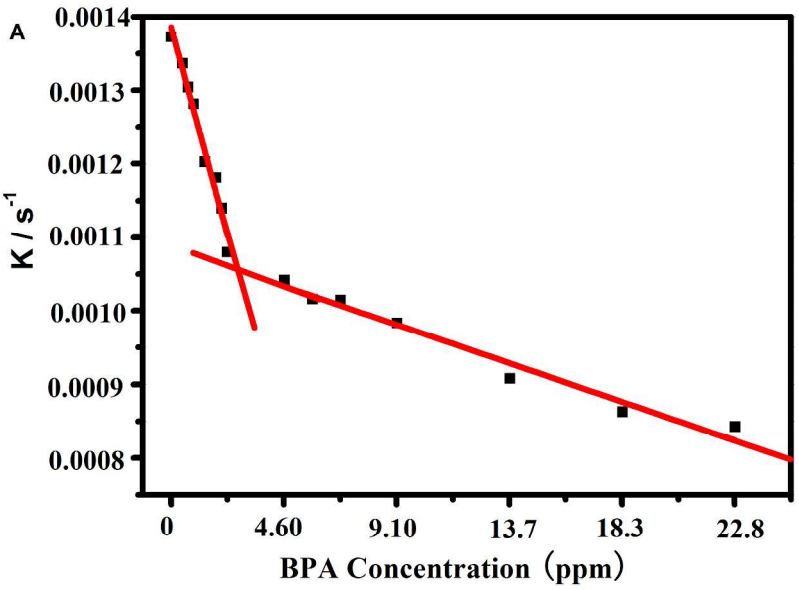

286x201mm (300 x 300 DPI)

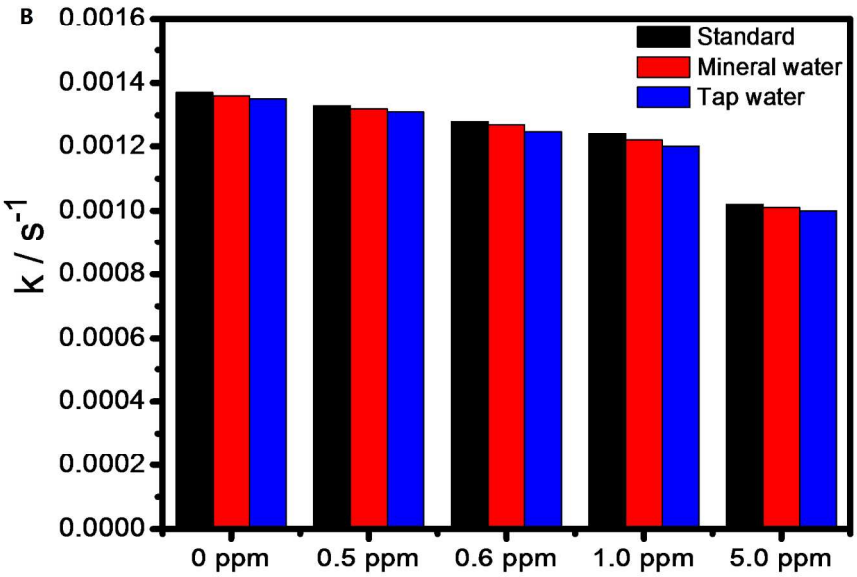

The relationship between the photoisomerization rate of SMIP (in standard sample, mineral water and tap water samples) and the BPA concentration from 0, 0.5, 0.6, 1.0, and 5.0 ppm
1230x922mm (96 x 96 DPI)